TELECONNECTION OF THE DOMINANT SPATIAL PATTERNS OF THE SEASONAL 500 hPa GPH FIELD

Zhang Mingli (章名立)

Institute of Atmospheric Physics, Academia Sinica, Beijing

Received August 6, 1987

ABSTRACT

The dominant spatial patterns of the seasonal 500 hPa GPH field is induced by the EOF analysis. In winter, the first and fourth eigenvector show that the PEA and PNA-like anomalous flow pattern will prevail when the temporal coefficient is negative. Through the variation of the temporal coefficient of the eigenvector, prevailing of these flow patterns is significantly related to the variation of SST in equatorial Pacific. These relationships are insignificant in other three seasons.

I. INTRODUCTION

The effect of tropical ocean on the variation of global climate is one of the major subjects in the study of air-sea interaction. Understanding of the relation between the interannual climate variation in tropical regions and the variation in tropical ocean has got remarkably advances. Statistical and dynamic studies (Horel and Wallace 1981; Hoskins and Karoly 1981) reveal a significant correlation between the variation of tropical ocean and the atmospheric circulation at mid-latitudes that happens during the north winter on the condition that westerlies are close to the equator. Therefore the planetary waves propagating along great circles are capable of carrying the signal from tropics to other locations at the globe under certain conditions. Some evidences have been found that during El Nino events in the tropical Pacific, it is in favor of some teleconnection patterns prevailing in northern midlatitudes, such as the PNA pattern in Pacific-North America (Horel and Wallace, 1981), the PEA pattern in Pacific-Eurasia (Zeng and Zhang, 1987) and the "seesaw" phenomenon between Greenland and Northern Europe (van Loon and Rogers, 1978). These flow patterns may lead to abnormal climate in certain areas. The 1976–1977 El Nino event was related to the severe cold winter in the southeast of the United States. During this period, the typical PNA pattern obviously prevailed. In 1970's, the cold summer disasters in Northeast China well responded to the El Nino in tropical Pacific (Zhang and Zeng, 1984, 1987), which might relate to the PEA pattern. However, the relationships between these teleconnection patterns and the behavior of tropical ocean have remained unknown. It is found that sometimes the reverse case may be seen. Fu et al. (1986), Diaz et al. (1987) pointed out that the PNA pattern did not appear in any of El Nino events. During 1972–1973 El Nino period, the situation was opposite to the PNA pattern. They suggested that the abnormal climate at mid-latitudes would be different according to the different warming pattern of the El Nino event.

The EOF analysis can reduce a series of original fields into a few principal fields, which can explain the main characters of the original fields. In this study, we use EOF method on the seasonal 500 hPa geopotential height anomaly field in Northern Hemisphere to separate the subordinate character of the GPH patterns and to distinguish the main mode of the anomalous flow patterns. Using the temporal series of the eigenvectors derived from the EOF analysis, we can further determine the correlation between these main GPH anomaly patterns and the variation of SST in tropical Pacific. In order to show seasonal variation, an analysis has been made for the four seasons respectively.

II. DATA AND ANALYSING METHOD

The data used in this study consist of (1) monthly 500 hPa geopotential height in Northern Hemisphere through June 1950 to May 1980, extracted from the magnetic tapes supplied by NCAR and (2) the time series of monthly SST anomalies through the same period along 130°W, 5° N–10°S, described by Pan and Oort (1983) as the key to the global climate.

The monthly data are compiled as the seasonal anomaly values, winter being December to February; spring, March to May; summer, June to August, and autumn, September to November. The selected grid interval is 20×10 degrees of longitude-latitude south of 80°N, and along 80°N circle, its interval is 30 degrees in longitude. Thus, it forms 118 grids north of 20°N in Northern Hemisphere. The data for seasonal anomalies of 500 hPa GPH are composed of four 118×30 matrices. The EOF technique is applied to these matrices. Table 1 shows the percentages of variance which can be explained by the first six eigenvectors for each seasons. The first eigenvector accounts for about 20% of the total variance and all the first four eigenvectors explain more than 50% of the total variance in each season.

Table 1. Percentage Variance of the Fisrt Six Eigenvectors for 500 hPa GPH Anomalies

No. of Eigenvector	I	II	III	IV	V	VI
Winter	19.7	34.9	47.2	57.8	67.7	73.3
Spring	27.8	41.2	50.1	57.0	63.1	68.9
Summer	20.5	34.3	44.5	51.8	57.8	62.8
Autumn	19.9	34.9	46.2	54.9	62.3	68.3

The relationship between the lags of the seasonal 500 hPa dominant patterns and the SST in equatorial Pacific is revealed by the correlation between the temporal coefficient of the first four eigenvectors of the seasonal GPH anomaly and the SST along equatorial 130° W which is "n" seasons previously. For example, for the winter GPH eigenvectors, the correlation coefficient value for lag=3 means that they are related with the SST in previous spring, and if lag equals −3, it means they are related with the SST in next autumn.

III. DOMINANT SPATIAL PATTERNS OF SEASONAL 500 hPa GPH ANOMALY FIELD

1. *Winter*

The spatial pattern of the first EOF eigenvector of 500 hPa GPH anomalies for winter consists of five main variability centers (Fig. 1a). These centers concentrate over North Atlantic to Eurasia sector, while over the sector from North Pacific to North America the variabilities are smaller. The most heavily weighted region is over Greenland. It shows oscillation of the GPH with those over central Atlantic and the British Isles, as the two centers have opposite signs. The former induces strengthening of westerlies over northern Atlantic when the anomalies over Greenland are negative. The latter consists of the

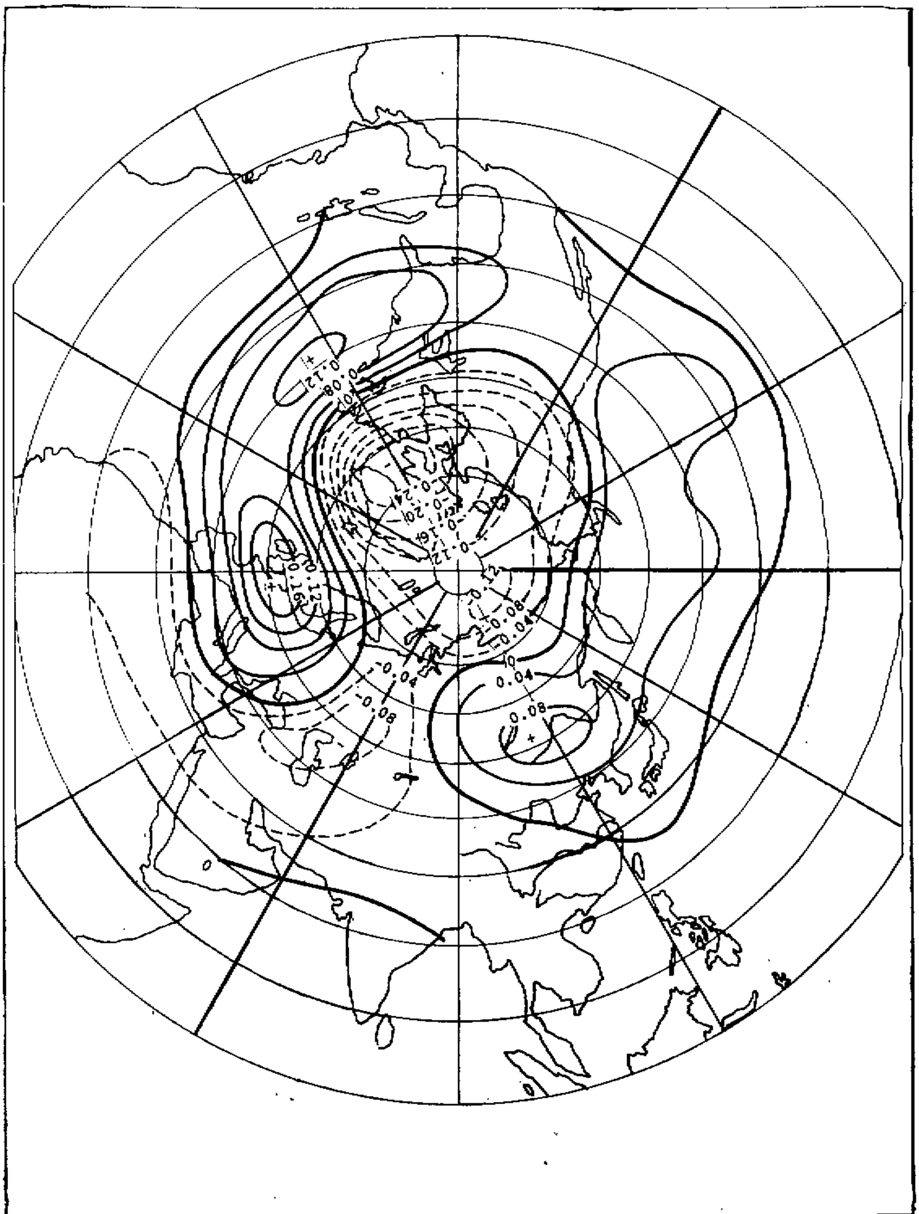

(a)

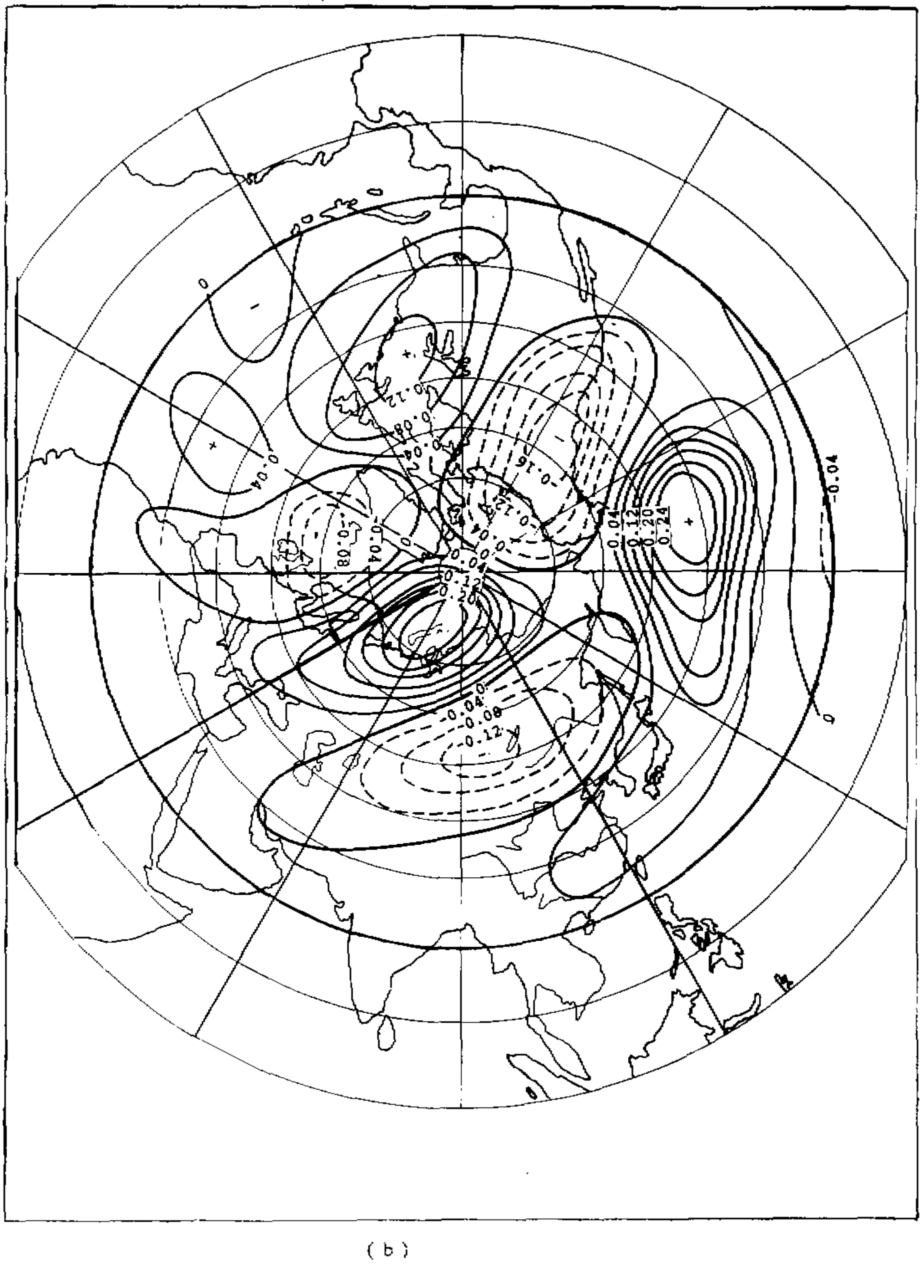

(b)

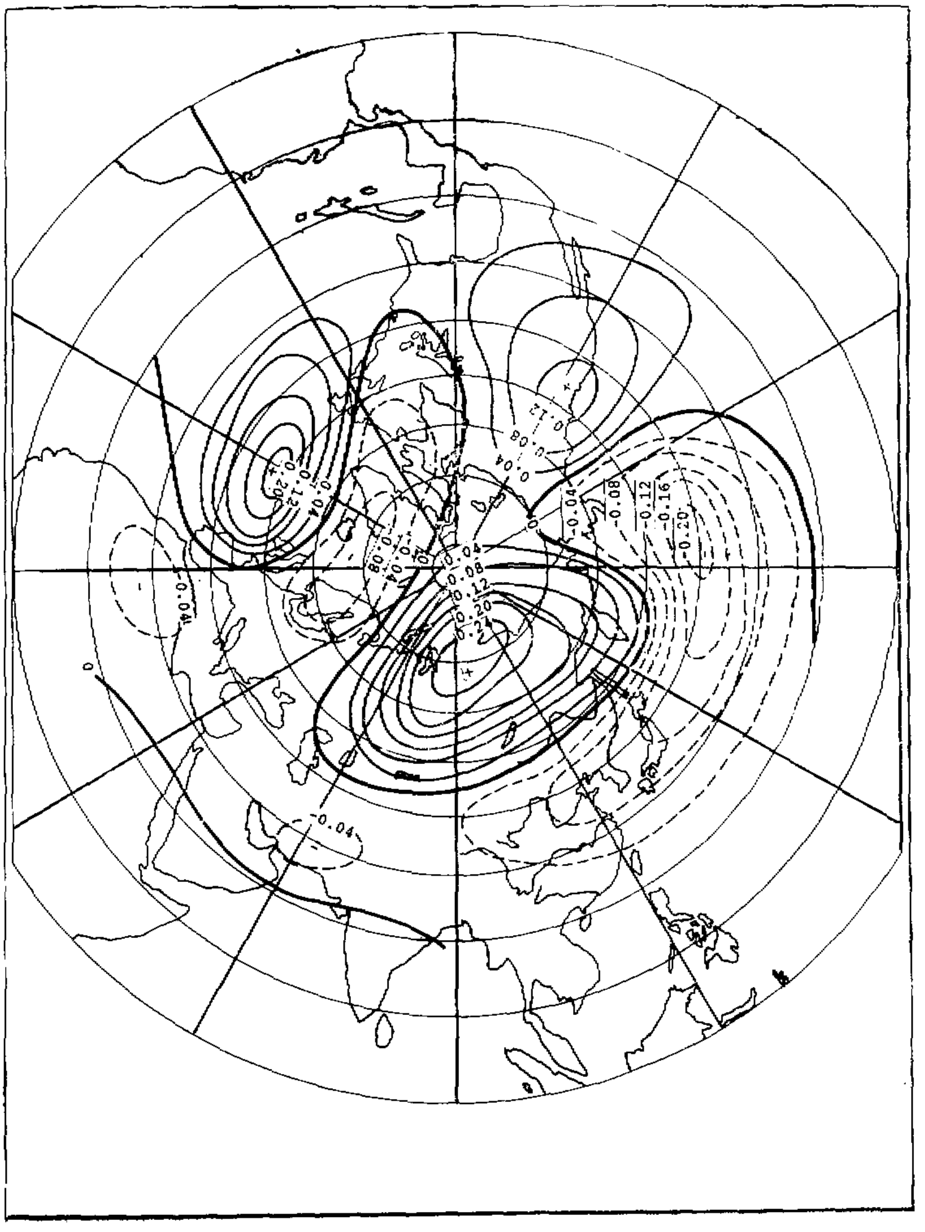

(c)

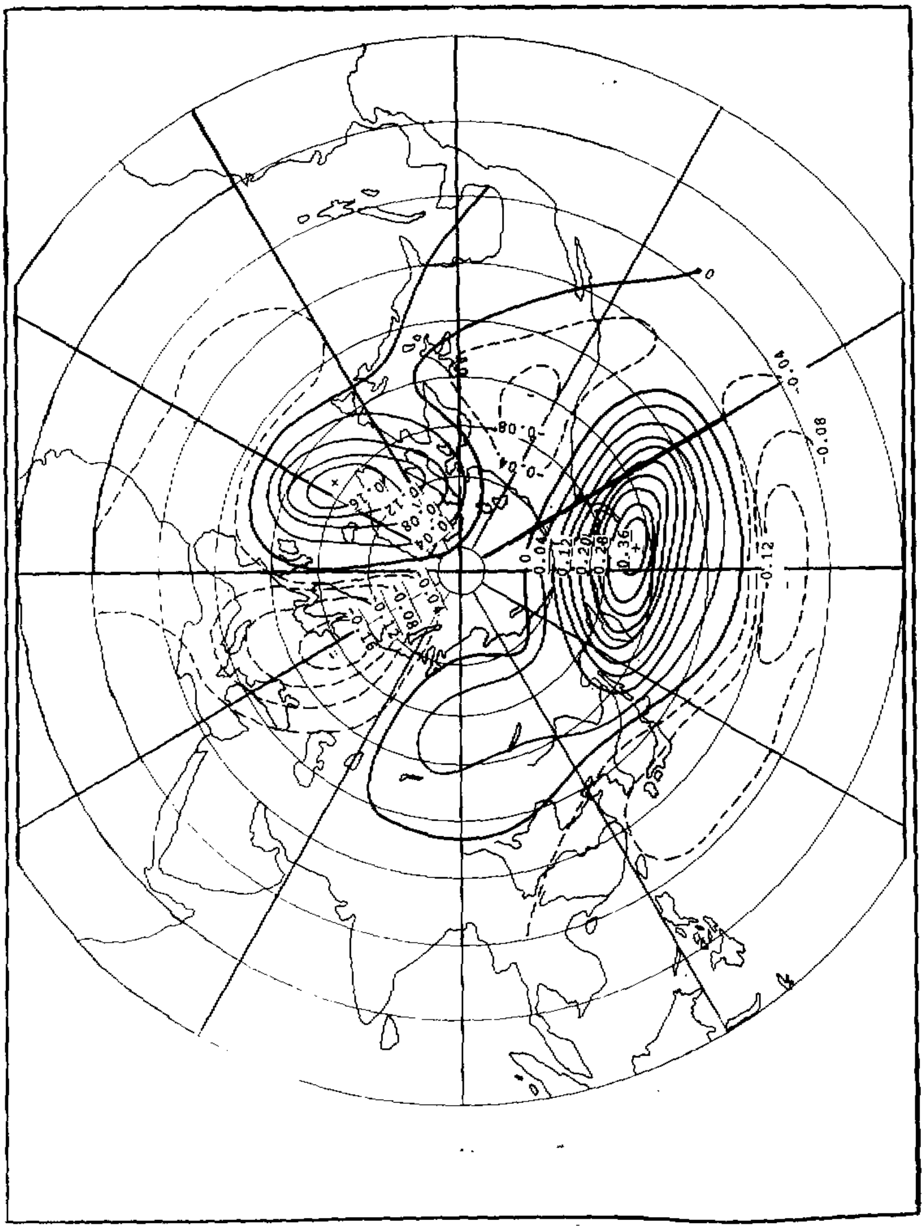

(d)

Fig. 1. The first four eigenvectors of 500 hPa GPH anomalies in winter for 1951–1980. (a) EOF I, (b) EOF II, (c) EOF III, (d) EOF IV,

"seesaw" phenomenon in response to the "seesaw" variation of surface air temperature between them. The centers over Eurasia show a train of standing wave. This wave relates to the development or decline of atmospheric planetary wave. When the temporal coefficient is negative, the anomalies over northeast Asia will be negative suggesting a deepened normal trough along the eastern coast of Asia. Meantime, the trough over western Europe and the ridge over the Caspian Sea will develop. It forms a trough-ridge-trough pattern over Eurasia, and coincides with the normal pattern of GPH field in winter. In comparison Fig. 1a with the correlation map between 500 hPa GPH anomalies and the SST along the equatorial 130°W during 1971–1980 (Zeng and Zhang 1987), the heavily weighted regions in Eurasia shown in Fig. 1a are just the regions in which the variation of geopotential height is significantly correlated with the SST along the equatorial 130°W. Zeng and Zhang (1987) suggested that during the period when tropical Pacific was relatively warm, it was possible that the PEA flow pattern would prevail in Eurasian regions. Fig. 1a depicts the dominant spatial pattern which can explain 20% of the total variance over 500 hPa having the characteristic of the PEA teleconnection pattern. This pattern has slightly differences from the EA pattern suggested by Wallace and Gutzler (1981), as the heavily weighted centers in Eurasia are of about 20 degrees of longitude west to the correlation centers of EA pattern. The coincidence of Fig. 1a with the correlation map by Zeng and Zhang (1987) indicates that the large scale interaction between the ocean in tropical Pacific and the atmosphere in middle latitude plays an important role in the circulation pattern in Eurasia. As the weights are weaker for the Pacific-North American sector, the first eigenvector relates to small changes there.

The spatial pattern of the second EOF eigenvector shows that there are three waves around the middle and higher latitude zones (Fig. 1b). The set of heavily weighted centers over Pacific-North America sector will result in the development of PNA flow pattern when the temporal coefficient is negative. The center over eastern Asia has an opposite sign to the center over eastern North America and the variation of the two major troughs along the eastern coasts of the two continents will go contrary. That is, one of them will develop while the other is filled up. Thus the character of the second eigenvector, which can explain 15.2% of the total variance, shows the development of planetary waves in the two continents may not be simultaneous.

The third eigenvector (Fig. 1c) mainly shows a pair of weighted centers in higher latitude: one is in Taymyr Peninsula, the other in Greenland sea. Another pair of centers in middle latitudes locates in western coast of Canada and central Pacific, which also shows a "seesaw" oscillation of geopotential height along a meridian.

The fourth eigenvector has greatest weight over the Aleutian Islands (Fig. 1d). South of this region, there is a vast area of opposite sign with a center near Hawaii. Connected with the variability centers over North America, the fourth eigenvector shows great similarity to the PNA pattern over eastern Pacific and North America; it explain 10% of total variance. Unlike the second eigenvector, the variation over East Asia is coherent to that over Aleutian and eastern part of North America, and the weights over there are weaker. In the North Atlantic sector, the variability centers coincide with the East Atlantic teleconnection pattern suggested by Wallace et al. (1981).

2. *Spring, Summer and Autumn*

Fig. 2a shows the spatial pattern of the first eigenvector in spring. In this chart, one of the principal characters is the teleconnection phenomenon of Wallace's Eurasia pattern. The other two heavily weighted regions are over the Buffin Islands and the central

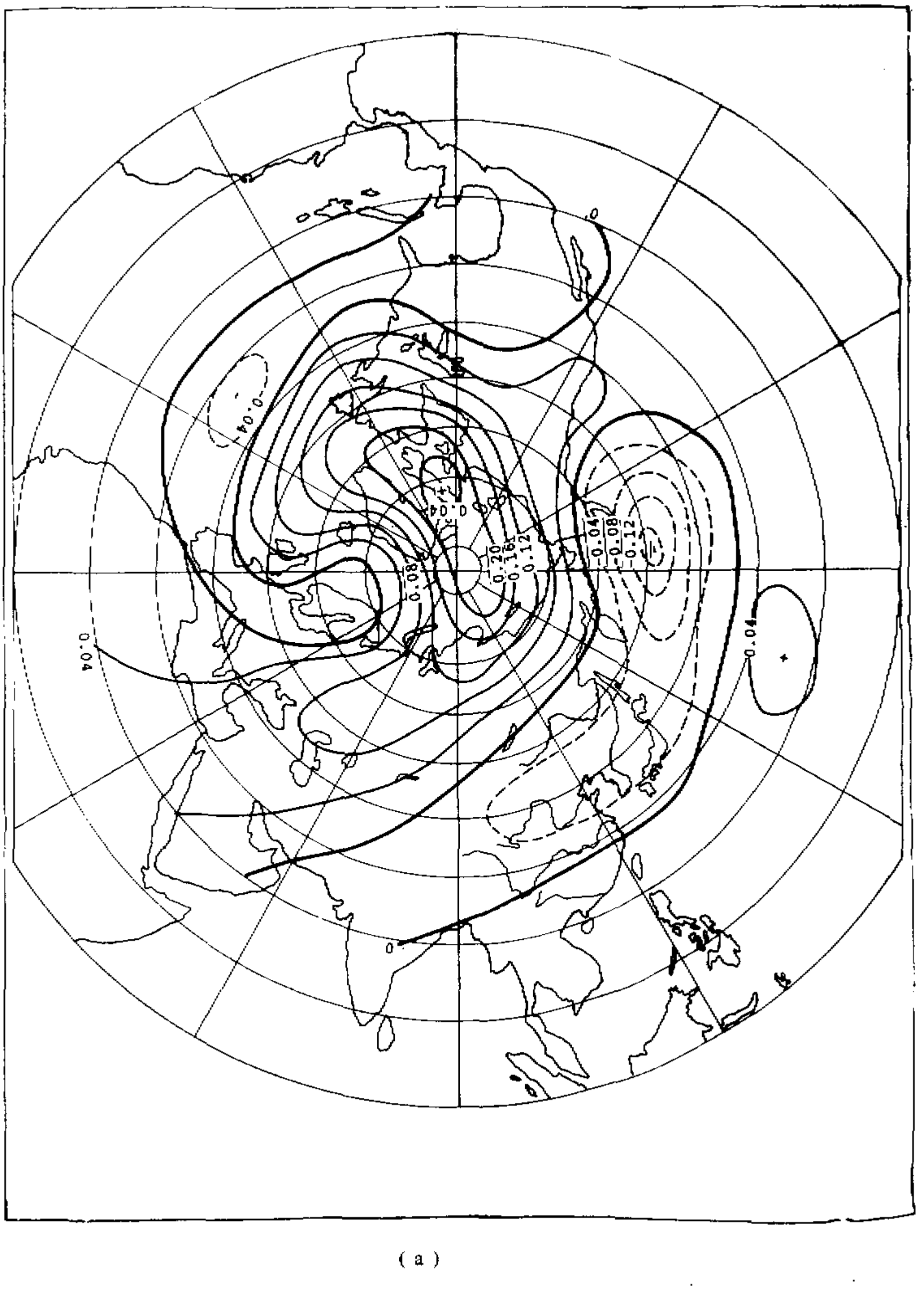

(a)

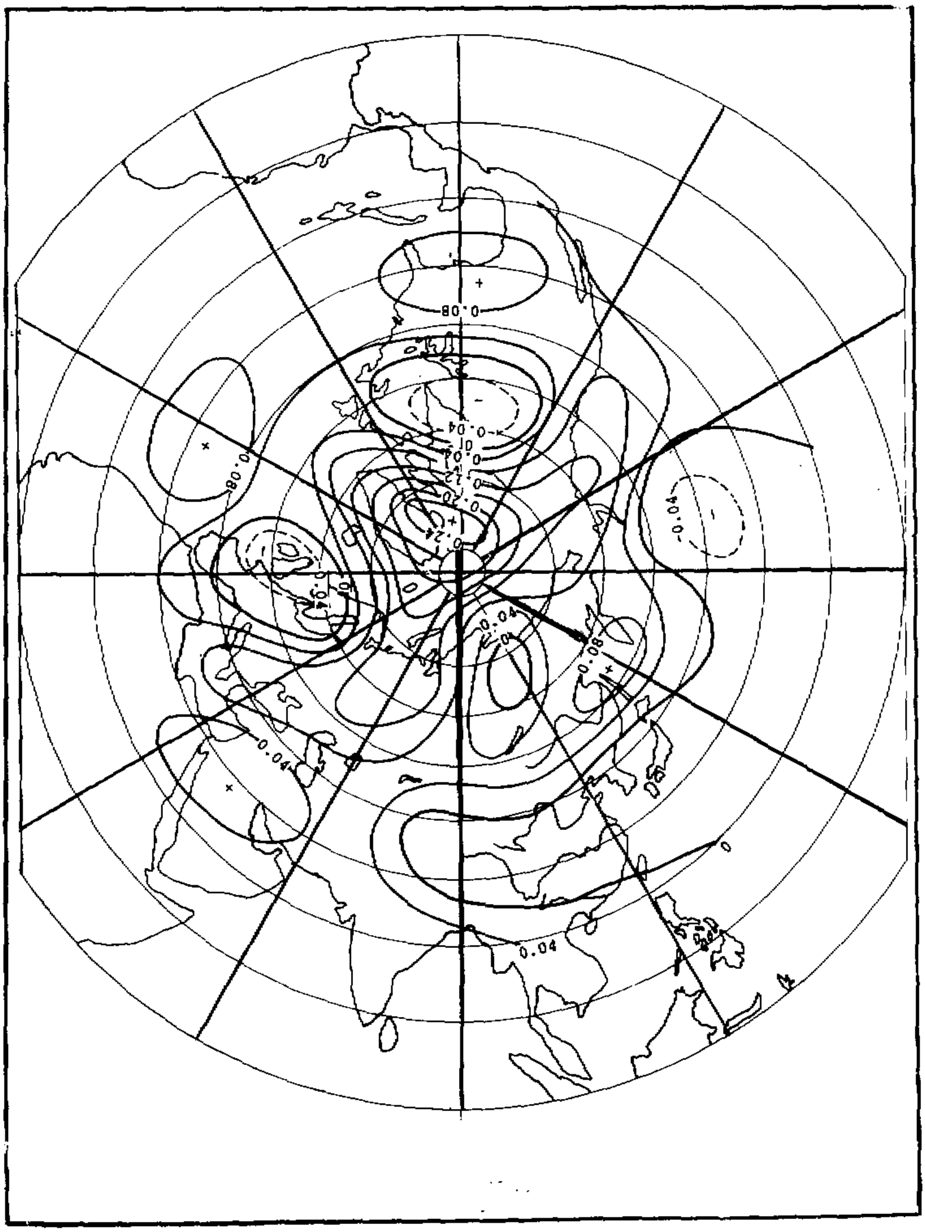

(b)

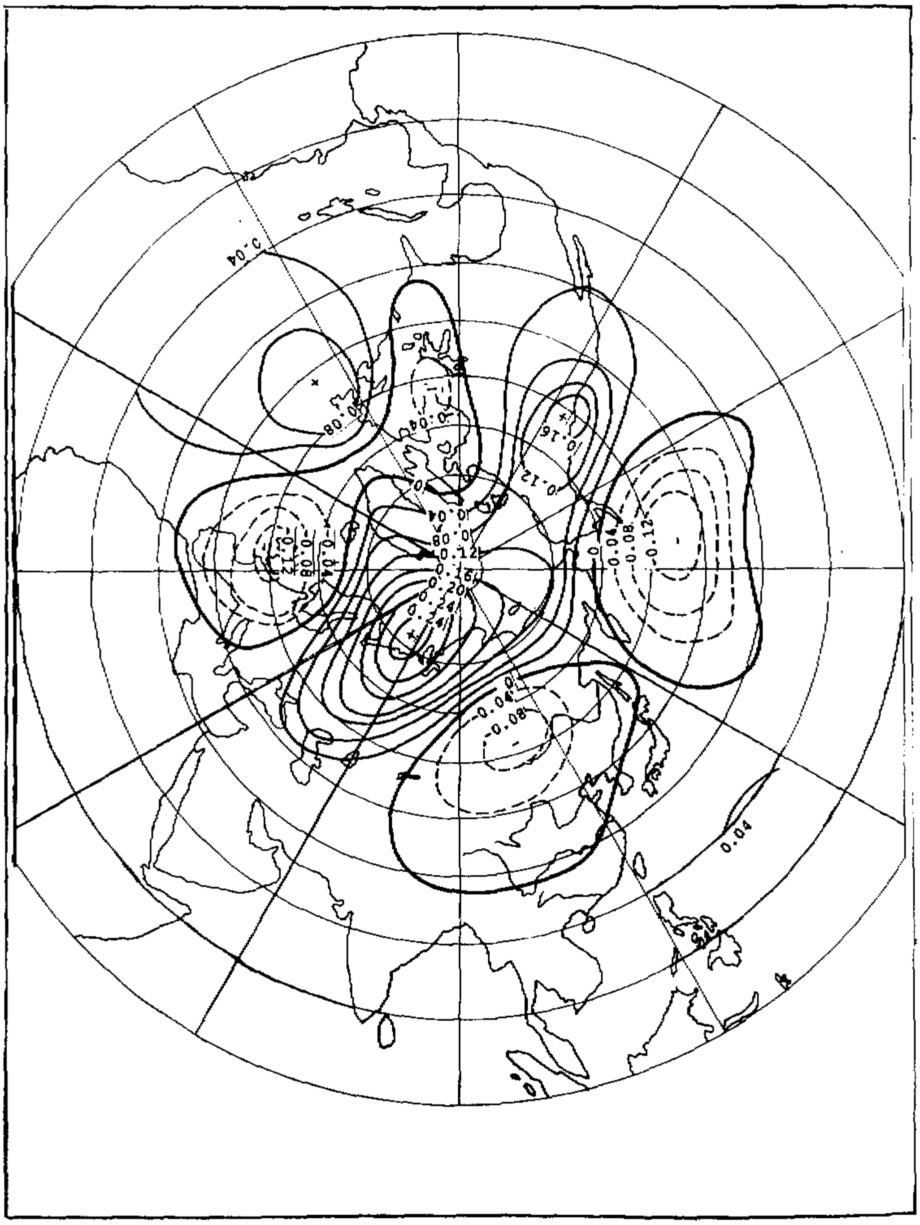

(c)

Fig. 2. The first eigenvectors of 500 hPa GPH anomalies in (a) spring, (b) summer and (c) autumn for 1950–1980.

Pacific. Each of them consists of a pair of centers with opposite signs of anomaly, by which a north-south oscillation of geopotential height over the Pacific or over the Atlantic will be formed.

The second eigenvector in spring has both the character of PNA pattern over North Pacific and North America region and "seesaw" phenomenon over Greenland and North Europe. The third and fourth eigenvectors only display a set of irregular centers (figures are not shown here).

The heavily weighted region in the first eigenvector during summer is formed in the Greenland area with the moderate coherent variations covering the Barents Sea, Alaska and the Sea of Okhotsk. At the middle and low latitudes the weights are smaller in general and split into a series of scattered centers. Thus, there has no significant teleconnection pattern in summer (Fig. 2b).

In autumn, the first eigenvector shows two heavily weighted regions in the Kara sea and the western coast of Canada (Fig. 2c). The variability centers over the Eurasia and over the Pacific-North America sector show the trace of PEA and PNA patterns. However, these patterns shift northward compared to those in winter. The second eigenvector in autumn mainly shows the standing wave of GPH anomalies along the meridian (figure omitted).

IV. TIME SERIES ANALYSIS OF THE TEMPORAL COEFFICIENTS OF EOF AND THEIR CORRELATIONS WITH THE SST IN EQUATORIAL PACIFIC

Through EOF analysis, we have seen that some teleconnection patterns appear in the dominant spatial patterns of 500 hPa GPH field. In the following, we will further analyse the time series of these EOF temporal coefficients.

Fig. 3 shows the time series of temporal coefficients of the first four eigenvectors of 500 hPa GPH field in winter. We also plot the time series of SST along equatorial Pacific (dashed line) in order to compare them with the variation of the EOF temporal coefficient of 500 hPa GPH field. As for the first eigenvetor, the temporal coefficients were out of phase for many years with the SST along equatorial Pacific. They were usually larger while the SST was in an extreme value with opposite sign.

In 1958, 1966, 1970, and 1977, the temporal coefficient reached relatively lower values. These four years were the El Nino years. The connection supported what Zeng and Zhang (1987) had suggested about the relationship between the prevailing PEA pattern in Eurasia and the El Nino events in equatorial Pacific. There were also contradictory condition for some years, especially in the winter of 1972–1973, when SST existed as an El Nino event in equatorial Pacific; the temporal coefficient was so large that the dominant character of 500 hPa wat contrary to PEA pattern. Fig. 4 shows the correlation coefficients of the temporal coefficients of the first four EOF eigenvectors with the SST in equatorial 130°W respectively. The correlation of the first eigenvector is significant at a 95% confidence level.

In Fig. 4, the correlation between the SST in equa orial Pacific and the temporal coefficient is also significant for the fourth eigenvector. Their correlation coefficient is even larger than that between SST and the temporal coefficient of the first eigenvector. In Fig. 3, the temporal coefficients were relatively small in 1954, 1958, 1961, 1964, 1966–1967, 1970, 1973, 1975 and 1977. Out of these nine years, seven were the El Nino years. Unlike the first eigenvector, the situation in the winter of 1972–1973 was still fit to this relations.

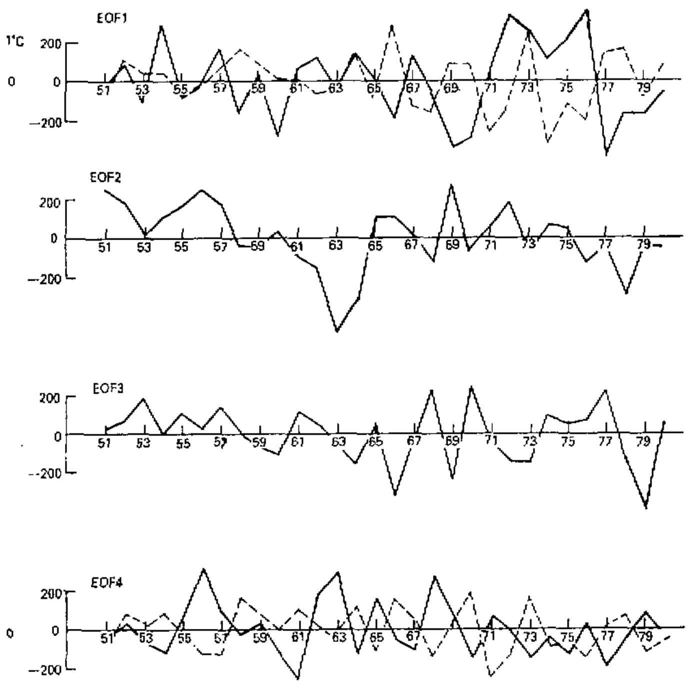

Fig. 3. Temporal coefficients of the first four eigenvectors of 500 hPa GPH anomalies in winter of 1951–1980.

As indicated above, the fourth eigenvector has the character of PNA flow pattern when the temporal coefficient is negative. In certain extent the significant correlation of temporal coefficient of the fourth eigenvector with variation of SST also indicates the relation of PNA pattern with the variation of SST. As the fourth eigenvector explains only 10% of total variance, the PNA pattern is sometimes obscure in the actual 500 hPa GPH field, and in the winter of 1972–1973, the actual 500 hPa GPH field even shows considerable difference from the PNA pattern.

The correlation of the temporal coefficients of the second and the third eigenvectors with the SST is insignificant (Fig. 4). The spatial mode of second eigenvector indicated above has the character of the PNA pattern. To analyse the temporal coefficients of second eigenvector (Fig. 3) in detail, the absolute values during the winters in 1957–1958, 1969–1970, 1972–1973 and 1976–1977 (these were El Nino years) were small. Thus the small values in amplitude induced a weak signal of PNA pattern in the second eigenvector although the second

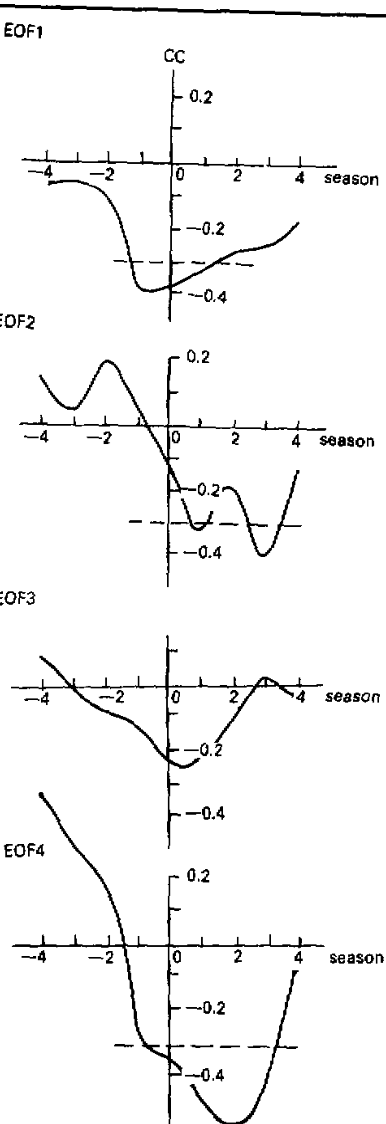

Fig. 4. Correlation coefficients between the temporal coefficients of the first four eigenvectors of 500 hPa GPH anomalies in winter and the seasonal SST anomalies along equatorial 130°W.

eigenvector explains 15% of total variance for the 500 hPa GPH field in winter.

Through the analysis of the EOF temporal coefficients, we may conclude that prevailing of PEA and PNA pattern in winter (as presented by the first and fourth eigenvectors, respectively) significantly relates with warming of SST in equatorial Pacific. The lag of correlation coefficient for the first eigenvector, which may be associated with the PEA pattern in Eurasia, equals −1 season. It implies that the variation of flow pattern over these areas leads to a variation of SST in equatorial Pacific. However, for the fourth eigenvector associated with the PNA pattern, the lag equals 2 seasons. It denotes clearly the delay of the variation in the atmosphere over Pacific-North America.

The correlation coefficients between the dominant patterns of 500 hPa GPH field in winter and the SST along equatorial Pacific show that the mechanism of air-sea interaction is different for Eurasia and North America. The variation signal of equatorial Pacific propagates along the westerlies and North America, as the lag of correlation equals 2 seasons between the temporal coefficient of the fourth eigenvector of 500 hPa GPH field and the time series of SST in tropical ocean. However, the lag of correlation for the first eigenvector equals −1 season. It may be considered that the variation of atmosphere in Eurasia will exert an influence on the strengthening of northeast monsoon in western Pacific in winter and then through the trade wind over tropical Pacific to the ocean.

The correlation coefficients of the first eigenvector both in spring and autumn with the SST in equatorial Pacific are insignificant (Fig. 6). Although the spatial patterns of the most important eigenvectors in spring and autumn show the characters of some teleconnection patterns as those in winter, the temporal coefficients do not indicate any considerable interaction between the prevailing flow pattern and the tropical ocean (Fig. 5).

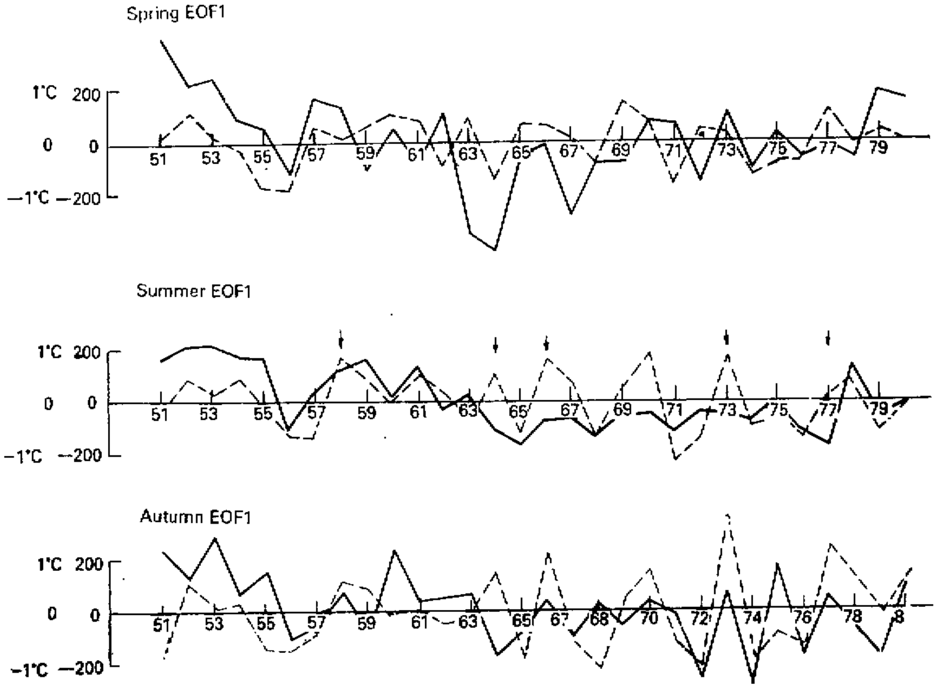

Fig. 5. Temporal coefficients of the first eigenvectors of 500 hPa GPH anomalies in spring, summer and autumn of 1950–1980.

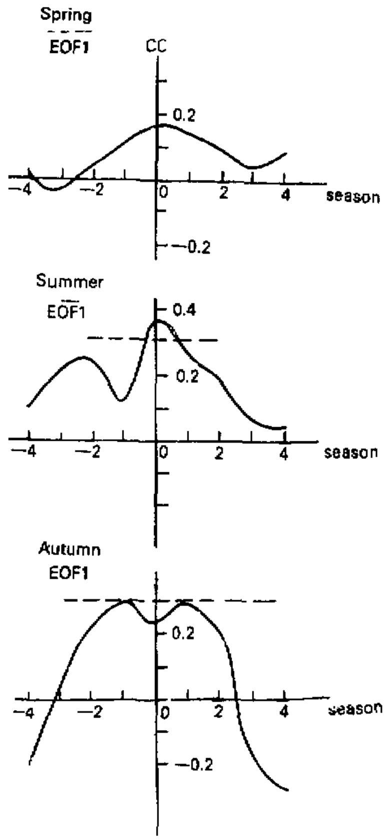

Fig. 6. Correlation coefficients between the temporal coefficients of the first eigenvectors of 500 hPa GPH anomalies in spring, summer and autumn and the seasonal SST anomalies along equatorial 130° W.

In summer season, the temporal coefficient of the first eigenvector (Fig. 5) has shown a drop since 1963 and kept negative values. Rogers et al. (1981) suggested that it might be due to the variation of atmospheric circulation rather than the systematic errors of objective analysis. Comparing with the obvious drop of the air temperature in summer since 1960 in Northern Hemisphere (Jones et al. 1982), we consider that the drop of the temporal coefficients of the first eigenvector in summer may be realistic. Thus the character of first eigenvector is mainly associated with the variaton of atmosphere in decade scale. The correlation with the SST in equatorial Pacific is significant only when lag=0.

V. CONCLUSION

Through the analysis of the dominant spatial pattern of the seasonal 500 hPa GPH anomaly fields and the correlation of these patterns with the sea surface temperature in equatorial Pacific, we get the following results:

(1) In winter, the PEA flow pattern and the "seesaw" phenomenon of geopotential

height between Greenland and the British Isles are the main teleconnection features of the first eigenvector of 500 hPa field. The second and fourth eigenvectors show the PNA-like pattern.

(2) The temporal coefficients of the first eigenvector in winter are out of phase with the SST in equatorial Pacific. The correlation coefficient between them is significant at a 95% confidence level. It indicates that the PEA pattern significantly relates to the El Nino event in equatorial Pacific. However, there appeared completely contradictory relation during 1972–1973 El Nino event.

(3) The correlation coefficient between the fourth eigenvector in winter and the SST in tropical Pacific reaches -0.56 at lag=2 seasons. The higher correlation shows the close relationship between the PNA pattern and the warm SST in equatorial Pacific. According to the temporal coefficients of the fourth eigenvector, the PNA pattern would be presented during the 1972–1973 El Nino event. As the fourth eigenvector explains only 10% of the total variance, the real resultant 500 hPa GPH field shows considerable difference from the PNA pattern in the winter of 1972–1973.

(4) The variation of the fourth EOF temporal coefficients lags in two seasons relative to the variation of the SST in equatorial Pacific. This may be attributed to the propagations of signal from tropical Pacific downstream to North America by westerlies. However, the variation of the first EOF temporal, coefficient leads in one season to a variation of the SST in equatorial Pacific. The mechanism of interaction between them is not clear, we may suppose that the variation of winter circulation over Eurasia may affect the strength of winter monsoon over western Pacific and then through the trade wind over the tropical Pacific to the ocean.

(5) The dominant spatial patterns in spring and autumn show the signal of teleconnection patterns as those shown in winter, but these patterns shift northward along with the seasonal movement of the westerlies. The eigenvector has no close relation with the SST in tropical Pacific.

(6) The dominant spatial pattern in summer has no significant teleconnection pattern in other seasons, and the first eigenvector shows the variation of atmospheric circulation of summer in decade scale.

REFERENCES

Diaz, H. F. & C. Fu (1987), "Climate in China and global climate", *Proceedings of the Beijing International Symposium on Climate* Oct. 30–Nov. 3, 1984 Beijing, China, 238–249, China Ocean Press, Beijing.

Fu, C., H. F. Diaz & J. O. Fletcher (1986), *Mon Wea. Rev.*, **114**: 1716–1738.

Horel, J. D. & J. M. Wallace (1981), *Mon. Wea. Rev.*, **109**: 813–829.

Hoskins. B. J. & D. J. Karoly (1981), *Jour. Atmos. Sci.*, **38**: 1179–1196.

Pan, Y. & A. H. Oort (1983), *Mon. Wea. Rev.*, **111**: 1244–1258.

Rogers, J. M. & D. S. Gutzler (1981), *Mon. Wea. Rev.*, **109**: 784–812.

Van Loon, H. & G. C. Rogers (1978), *Mon. Wea. Rev.*, **106**: 296–310.

Zeng, Z. & M. Zhang (1987), "Climate in China and global climate", Proceedings of the Beijing International Symposium on Climate Oct. 30–Nov. 3, 1984 Beijing, China, 250–263, China Ocean Press.

Zhang, M. & Z. Zeng (1984), *Tropical ocean-atmosphere newsletter*, **23**: 5–7.

Zhang, M., Z. Zeng & Y. Pan (1987), "Climate in China and global climate", *Proceedings of the Beijing International Symposium on Climate* Oct, 30–Nov. 3, 1984 Beijing, China, 226–237, China Ocean Press,